

Rudolf Holze and Yuping Wu

Electrochemical Energy Conversion and Storage

An Introduction

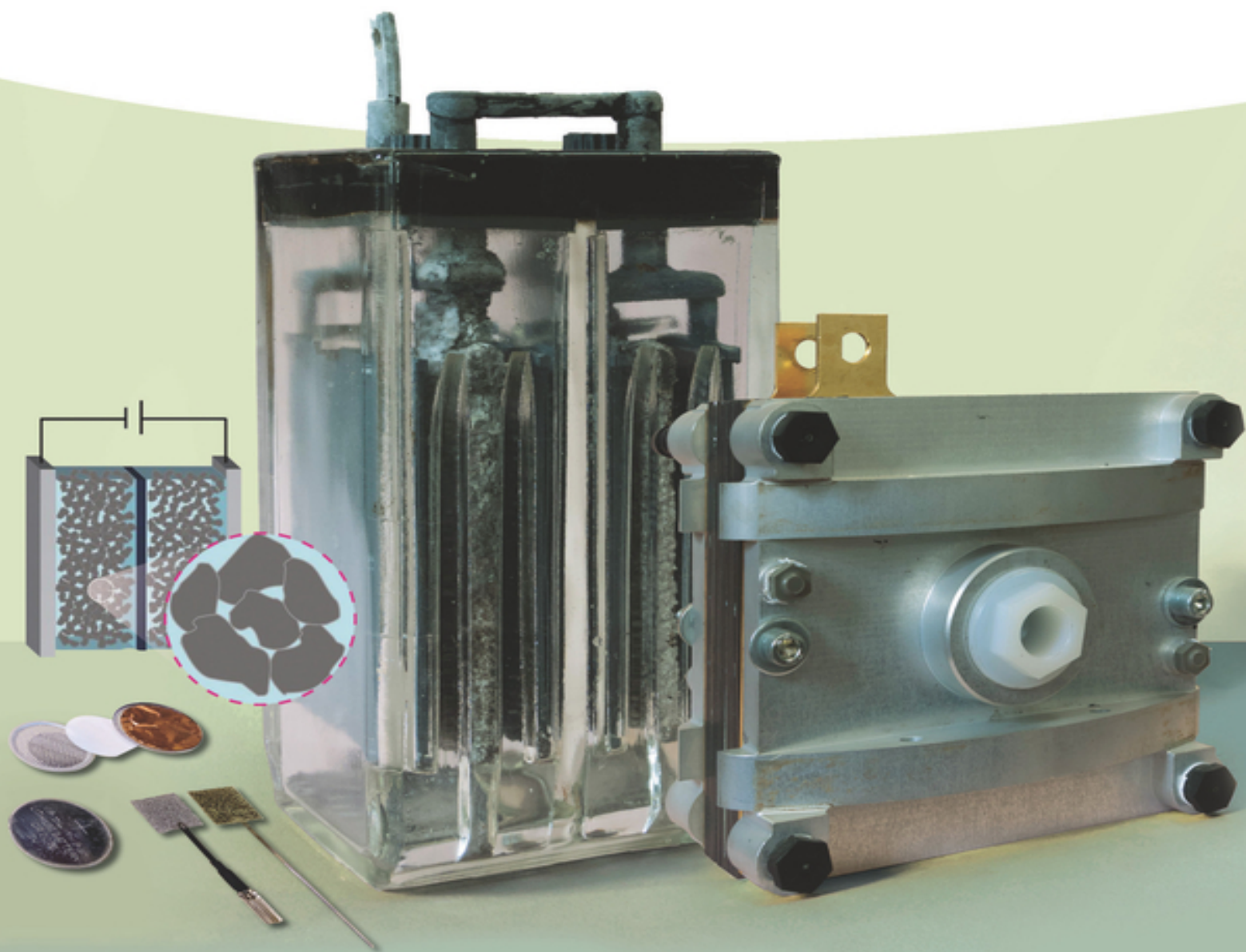


Table of Contents

[Cover](#)

[Title Page](#)

[Copyright](#)

[Foreword](#)

[Preface](#)

[1 Processes and Applications of Energy Conversion and Storage](#)

[Notes](#)

[2 Electrochemical Processes and Systems](#)

[2.1 Parasitic Reactions](#)

[2.2 Self-discharge](#)

[2.3 Device Deterioration](#)

[3 Thermodynamics of Electrochemical Systems](#)

[Notes](#)

[4 Kinetics of Electrochemical Energy Conversion Processes](#)

[4.1 Steps of Electrode Reactions and Overpotentials](#)

[4.2 Transport](#)

[4.3 Charge Transfer](#)

[4.4 Overpotentials](#)

[4.5 Diffusion](#)

[4.6 Further Overpotentials](#)

[Note](#)

[5 Electrodes and Electrolytes](#)

[5.1 Recycling](#)

Notes

6 Experimental Methods

6.1 Battery Tester

6.2 Current-Potential Measurements

6.3 Charge/Discharge Measurements

6.4 Battery Charging

6.5 Linear Scan and Cyclic Voltammetry

6.6 Impedance Measurements

6.7 Galvanostatic Intermittent Titration Technique (GITT)

6.8 Potentiostatic Intermittent Titration Technique (PITT)

6.9 Step Potential Electrochemical Spectroscopy (SPECS)

6.10 Electrochemical Quartz Crystal Microbalance (EQCM)

6.11 Non-electrochemical Methods

Notes

7 Primary Systems

7.1 Aqueous Systems

7.2 Nonaqueous Systems

7.3 Metal-Air Systems

7.4 Reserve Batteries¹

Note

8 Secondary Systems

8.1 Aqueous Systems

8.2 Nonaqueous Systems

8.3 Gel Polymer Electrolyte-based Secondary Batteries

[8.4 Solid Electrolyte-based Secondary Batteries](#)

[8.5 Rechargeable Metal-Air Batteries](#)

[8.6 High-Temperature Systems](#)

[9 Fuel Cells](#)

[9.1 The Oxygen Electrode](#)

[9.2 The Hydrogen Electrode](#)

[9.3 Common Features of Fuel Cells](#)

[9.4 Classification of Fuel Cells](#)

[9.5 Applications of Fuel Cells](#)

[9.6 Fuel Cells in Energy Storage Systems](#)

[Notes](#)

[10 Flow Batteries¹](#)

[10.1 The Iron/Chromium System](#)

[10.2 The Iron/Vanadium System](#)

[10.3 The Iron/Cadmium System](#)

[10.4 The Bromine/Polysulfide System](#)

[10.5 The All-Vanadium System](#)

[10.6 The Vanadium/Bromine System](#)

[10.7 Actinide RFBs](#)

[10.8 All-Organic RFBs](#)

[10.9 Nonaqueous RFBs](#)

[10.10 Hybrid Systems](#)

[10.11 The Zinc/Cerium System](#)

[10.12 The Zinc/Bromine System](#)

[10.13 The Zinc/Organic System](#)

[10.14 The Cadmium/Organic System](#)

[10.15 The Lead/Lead Dioxide System](#)

[10.16 The Cadmium/Lead Dioxide System](#)

[10.17 The All-Copper System](#)

[10.18 The Zinc/Nickel System](#)

[10.19 The Lithium/LiFePO₄ System](#)

[10.20 Vanadium Solid-Salt Battery](#)

[10.21 Vanadium-Dioxygen System](#)

[10.22 Electrochemical Flow Capacitor](#)

[10.23 Current State and Perspectives](#)

[Notes](#)

[11 Supercapacitors](#)

[11.1 Classification of Supercapacitors](#)

[11.2 Electrical Double-Layer Capacitors](#)

[11.3 Pseudocapacitors](#)

[11.4 Hybrid Capacitors](#)

[11.5 Testing of Supercapacitors](#)

[11.6 Commercially Available Supercapacitors](#)

[11.7 Application of Supercapacitors](#)

[Appendix](#)

[Symbols](#)

[Acronyms, Terms, and Definitions](#)

[Further Reading](#)

[Chapter 1: Processes and Applications of Energy Conversion and Storage](#)

[Chapter 2: Electrochemical Processes and Systems: Classification, Typical Properties and Applications, Hybrid Types](#)

[Chapter 3: Thermodynamics of Electrochemical Systems](#)

[Chapter 4: Kinetics of Electrochemical Energy Conversion Processes](#)

[Chapter 5: Electrodes and Electrolytes](#)

[Chapter 6: Experimental Methods](#)

[Chapter 7: Primary Systems](#)

[Chapter 8: Secondary Systems](#)

[Chapter 9: Fuel Cells](#)

[Chapter 10: Flow Batteries](#)

[Chapter 11: Supercapacitors](#)

[Index](#)

[End User License Agreement](#)

List of Tables

Chapter 1

[Table 1.1 Development and performance targets for grid-related storage.](#)

[Table 1.2 Comparison of some energy storage systems for e.g. utility transmi...](#)

[Table 1.3 Sustainability profiles of selected processes relevant in energy c...](#)

[Table 1.4 Volumetric and gravimetric energy densities of selected energy sto...](#)

[Table 1.5 Advantages and disadvantages of energy carriers.](#)

[Table 1.6 Use of hydrogen in energy storage and distribution concepts.](#)

[Table 1.7 Relative importance of system properties for selected applications...](#)

Chapter 2

[Table 2.1 Selected characteristics of electric energy storage systems.](#)

[Table 2.2 Popular consumer-type primary batteries.](#)

[Table 2.3 Typical features of batteries in common sizes.](#)

[Table 2.4 Battery sizes and applications.](#)

[Table 2.5 Self-discharge rates at room temperature.](#)

Chapter 3

[Table 3.1 Electrode reactions in aqueous solution, free enthalpies, and elec...](#)

[Table 3.2 Coulombic capacity \$Q\$ and characteristic data of selected electrode ...](#)

[Table 3.3 Coulombic capacity \$Q\$ and characteristic data of selected electrode ...](#)

Chapter 4

[Table 4.1 Kinetic data of selected battery electrode materials.](#)

Chapter 5

[Table 5.1 Tasks of phase I in an electrode.](#)

[Table 5.2 Modes of electrode material operation and associated common featur...](#)

[Table 5.3 Tasks of phase II in an electrode.](#)

[Table 5.4 Metal content in wt% for selected types of batteries.](#)

Chapter 7

[Table 7.1 History of selected primary batteries.](#)

[Table 7.2 Tunnel sizes of different crystal phases of \$\text{MnO}_2\$.](#)

[Table 7.3 Some physicochemical properties of selected metals.](#)

[Table 7.4 Selected properties of lithium metal.](#)

[Table 7.5 Some parameters of primary lithium batteries.](#)

[Table 7.6 Some physical parameters of three active materials studied as posi...](#)

[Table 7.7 Some properties of metal-air primary batteries.](#)

[Table 7.8 Some characteristics of Zn//air batteries.](#)

Chapter 9

[Table 9.1 Dioxygen reactions in electrochemical energy technology.](#)

Chapter 10

[Table 10.1 Data of selected redox flow batteries.](#)

[Table 10.2 Comparison of electrochemical storage technologies competing with...](#)

Chapter 11

[Table 11.1 Comparison between supercapacitors and lithium-ion batteries.](#)

[Table 11.2 Electrochemical windows for some typical electrolytes.](#)

[Table 11.3 Some characteristics of MnO₂-based pseudocapacitors with neutral ...](#)

[Table 11.4 Comparison of the three types of pseudocapacitors based on conduc...](#)

[Table 11.5 Selected characteristics of some hybrid capacitors.](#)

[Table 11.6 Advantages and challenges for supercapacitors.](#)

List of Illustrations

Chapter 1

[Figure 1.1 Battery-operated vehicle \(Krüger, Berlin, Germany\) of 1899.](#)

[Figure 1.2 Battery-operated car built by R. Slaby around 1919.](#)

[Figure 1.3 Actual power delivery from a wind farm \(76 turbines\) in Chap-Chat...](#)

[Figure 1.4 Power outages in minute\(s\) per year in 2013 in Europe.](#)

[Figure 1.5 Primary energy sources in electric energy production 1973, total ...](#)

[Figure 1.6 Primary energy sources in electric energy production in 2005.](#)

[Figure 1.7 Primary energy sources in electric energy production in 2014, tot...](#)

[Figure 1.8 Typical discharge times and rated powers of electrochemical stora...](#)

[Figure 1.9 Schematic display of contributions from various operating reserve...](#)

[Figure 1.10 Storage capacity and typical discharge times of various storage ...](#)

[Figure 1.11 Gravimetric and volumetric energy densities of common storage ma...](#)

[Figure 1.12 Theoretical gravimetric and volumetric energy densities of selec...](#)

[Figure 1.13 Driving ranges of a car running on different energy storage syst...](#)

[Figure 1.14 Options of hydrogen generation and utilization.](#)

[Figure 1.15 Performance index \(in % with a higher percentage implying better...](#)

[Figure 1.16 Gravimetric power and energy densities of secondary electrochemi...](#)

Chapter 2

[Figure 2.1 Simplified schemes of devices for electrochemical energy storage ...](#)

[Figure 2.2 Distinguishing a capacitor from an accumulator.](#)

[Figure 2.3 Options of serial hybrids.](#)

[Figure 2.4 Fractions of various battery systems in the total of 42 531 tons ...](#)

[Figure 2.5 Revenue distribution for the global battery market in 2009.](#)

[Figure 2.6 Extrapolated annual capacity losses of selected primary and secon...](#)

[Figure 2.7 New \(a\), degraded \(b\), and reconditioned cadmium electrode \(c\).](#)

[Figure 2.8 Corroded zinc cans of zinc-carbon batteries.](#)

Chapter 3

[Figure 3.1 Scheme of an electrochemical cell \(primary battery: alkaline cell...](#)

[Figure 3.2 pH dependency of electrode potentials.](#)

[Figure 3.3 Discharge curves of a lead-acid cell at different discharge rates...](#)

Chapter 4

[Figure 4.1 Reaction steps for the cadmium electrode in a nickel-cadmium accu...](#)

[Figure 4.2 Concentration gradients at the metal/solution interface with bulk...](#)

[Figure 4.3 Current versus time gradients during ongoing flow of current.](#)

[Figure 4.4 Current density versus charge transfer overpotential plots of a p...](#)

[Figure 4.5 Tafel plot for a one-electron charge transfer reaction with \$\alpha\$...](#)

[Figure 4.6 Current-potential relationship of a silver wire electrode in an a...](#)

[Figure 4.7 Volumetric energy density of selected primary and secondary syste...](#)

[Figure 4.8 Available capacity of a 120 Ah battery at different Peukert numbe...](#)

[Figure 4.9 Rated and actually delivered capacities for selected systems.](#)

[Figure 4.10 Ragone plot for selected electrochemical systems. Labels: discha...](#)

[Figure 4.11 Radar plot for seven fictional different batteries with differen...](#)

Chapter 5

[Figure 5.1 Phases I and II and an interface or interphase of an electrode wi...](#)

[Figure 5.2 Schematic structure of the electrochemical double layer as sugges...](#)

[Figure 5.3 Electrode terminology.](#)

[Figure 5.4 Nanostructured \$\text{MnO}_2\$ -\(a\) and \$\text{Mn}_3\text{O}_4\$ -\(b\). to be used in a supercapaci...](#)

[Figure 5.5 Theoretical gravimetric and volumetric charge densities of select...](#)

[Figure 5.6 Volume changes and theoretical gravimetric charge densities of se...](#)

[Figure 5.7 Operating principle of the “rocking-chair” lithium-ion battery.](#)

[Figure 5.8 Schematic display of electrode potentials of typical electrode ma...](#)

[Figure 5.9 Trends of properties and material behavior in various application...](#)

[Figure 5.10 Hybrid battery with three compartments.](#)

[Figure 5.11 Hybrid battery with three compartments.](#)

Chapter 6

[Figure 6.1 Simple battery testers.](#)

[Figure 6.2 Scheme of the experimental setup for measuring a current density ...](#)

[Figure 6.3 Galvanostatic current versus electrode potential curve of a plati...](#)

[Figure 6.4 Galvanostatic current versus electrode potential curve of a lead ...](#)

[Figure 6.5 Potentiostatic setup based on an operational amplifier with a vol...](#)

[Figure 6.6 Potentiostatic current density versus electrode potential curve o...](#)

[Figure 6.7 Current versus cell voltage curve of a nickel-metal hydride accum...](#)

[Figure 6.8 Current versus cell voltage curve of a nickel-metal hydride accum...](#)

[Figure 6.9 Discharge curves of a nickel-cadmium accumulator with a nominal c...](#)

[Figure 6.10 Discharge curves of a nickel-cadmium accumulator size AAA of nom...](#)

[Figure 6.11 Discharge curves of a nickel-metal hydride accumulator size AAA ...](#)

[Figure 6.12 Discharge curves of a nickel-metal hydride accumulator size AAA ...](#)

[Figure 6.13 Discharge curve of a nickel-metal hydride accumulator size AAA \(...](#)

[Figure 6.14 Charge/discharge curves of a nickel-metal hydride accumulator si...](#)

[Figure 6.15 Charge/discharge curves of a lithium-ion accumulator type CR2031...](#)

[Figure 6.16 Charge/discharge curves of a lithium-ion accumulator type CR2031...](#)

[Figure 6.17 Cell voltage under load of a cell with a passivated electrode; 1...](#)

[Figure 6.18 Charging curve of an electrolytic capacitor of 2200 \$\mu\$ F capacitan...](#)

[Figure 6.19 Charge and discharge curves of a supercap with \$C = 10\$ F.](#)

[Figure 6.20 Battery chargers: Top left: Charger for lithium button cells. Ce...](#)

[Figure 6.21 Lifetime performance of a lithium-ion battery as a function of t...](#)

[Figure 6.22 Voltage and current profiles during charging a lead-acid battery...](#)

[Figure 6.23 Voltage and current profiles during charging a lithium-ion batte...](#)

[Figure 6.24 Charging current as a function of time of a nickel-cadmium accum...](#)

[Figure 6.25 Potential versus time protocols for linear sweep voltammetry \(LS...](#)

[Figure 6.26 LSV plot of a nickel wire in contact with an aqueous electrolyte...](#)

[Figure 6.27 LSV plot of a nickel foam electrode in contact with an aqueous e...](#)

[Figure 6.28 CV plot of a lead wire in contact with aqueous electrolyte solut...](#)

[Figure 6.29 CV of the redox system \$\text{Fe}^{2+}/\text{Fe}^{3+}\$, single cyclic scan at ...](#)

[Figure 6.30 Measured impedance data of a platinum working electrode in an aq...](#)

[Figure 6.31 Randles equivalent circuit. Randles originally represented the c...](#)

[Figure 6.32 Equivalent circuit for a redox electrode reaction.](#)

[Figure 6.33 Simulated electrode impedance with a Warburg diffusion element \(...\)](#)

[Figure 6.34 Equivalent circuit with a constant phase element representing th...](#)

[Figure 6.35 Measured impedance data of a platinum working electrode in an aq...](#)

[Figure 6.36 Simple equivalent circuit of a battery.](#)

[Figure 6.37 Simple partially expanded equivalent circuit of a battery.](#)

[Figure 6.38 Cell impedance of an alkaline button cell type AG13.](#)

[Figure 6.39 Voltage and potential transients recorded during a GITT experime...](#)

[Figure 6.40 Potential transients of the negative electrode recorded during a...](#)

[Figure 6.41 Thevenin equivalent circuit model.](#)

[Figure 6.42 Components of a modeling situation.](#)

[Figure 6.43 Modeling a battery.](#)

Chapter 7

[Figure 7.1 Typical discharge curve of a zinc-carbon battery using 5 M \$\text{NH}_4\text{Cl}\$...](#)

[Figure 7.2 Typical discharge curve of a \$\text{Zn//MnO}_2\$ alkaline battery at room te...](#)

[Figure 7.3 Leaking alkaline battery.](#)

[Figure 7.4 Discharge curves of a R20 \$\text{Zn//HgO}\$ battery at 20 °C with different...](#)

[Figure 7.5 Discharge curves of a \$\text{Zn//AgO}\$ battery at room temperature.](#)

[Figure 7.6 \(a\) Ionic conductivities at different temperature and \(b\) freezin...](#)

[Figure 7.7 Discharge curves of an open \$\text{Cd//AgO}\$ battery at room temperature....](#)

[Figure 7.8 Discharge curve of \$\text{Mg//MnO}_2\$ primary battery at room temperature: ...](#)

[Figure 7.9 Comparison of some primary batteries during storage.](#)

[Figure 7.10 Discharge curves of a coin-type Li//MnO₂ battery at different ou...](#)

[Figure 7.11 Discharge curves of a coin-type Li//Pb₂Bi₂O₅ battery with nomina...](#)

[Figure 7.12 Discharge curves of a cylindrical R6-type Li//CuO battery at dif...](#)

[Figure 7.13 Discharge curve of Ag₂V₄O₁₁ nanowires.](#)

[Figure 7.14 Discharge curves of an R20-type Li//CuS primary battery with nom...](#)

[Figure 7.15 Discharge curves of a Li//FeS₂ primary battery at different temp...](#)

[Figure 7.16 Discharge curve of a Li//CF_x primary battery at different temper...](#)

[Figure 7.17 The discharge properties of the Li/I₂: LiI\(HPN\)₂ film paper batte...](#)

[Figure 7.18 Typical discharge curves of Li//SO₂ battery at different tempera...](#)

[Figure 7.19 Typical discharge curves of a disk Li//SOCl₂ primary battery wit...](#)

[Figure 7.20 Discharge curves at 20 °C for D-type \(a\) Li//BCX and \(b\) Li//CSC...](#)

[Figure 7.21 Discharge curves of a Mg//air battery at a constant current of 0...](#)

[Figure 7.22 Discharge curves for three Al//air batteries: \(a\) gel electrolyt...](#)

[Figure 7.23 Discharge curves of a Zn//air primary battery of 20 Ah at differ...](#)

[Figure 7.24 Discharge curve of Fe-B alloy at 100 mAh g⁻¹ in 30% KOH so...](#)

[Figure 7.25 Discharge curves of Li//air primary batteries at 0.1 mA cm⁻²...](#)

[Figure 7.26 Vertical cross-section of an aluminum-air battery.](#)

Chapter 8

[Figure 8.1 Positive \(a\) and negative \(b\) electrode grids of a starter batter...](#)

[Figure 8.2 Relationship between resistance and density of H₂SO₄ solution.](#)

[Figure 8.3 Discharge curves of a lead-acid battery with capacity of 1380 Ah ...](#)

[Figure 8.4 Cutoff charging/discharging voltage of batteries containing diffe...](#)

[Figure 8.5 Low-speed electric vehicle running on the road in China.](#)

[Figure 8.6 Typical discharge curve of a Ni-Cd battery at 30 °C.](#)

[Figure 8.7 Schematics of gas transport during overcharge \(a\) and polarity re...](#)

[Figure 8.8 Discharge curves of a Ni-H₂ battery at different temperature.](#)

[Figure 8.9 Effects of discharge rate on useful capacity percentage.](#)

[Figure 8.10 Typical galvanostatic charge/discharge curve for a sealed Ni-Fe ...](#)

[Figure 8.11 \(a\) Charge/discharge curves and \(b\) cycling performance of a Ni-...](#)

[Figure 8.12 Cycling behavior of \(a\) macroporous \$\text{LiMn}_2\text{O}_4\$ in 0.5 M \$\text{Li}_2\text{SO}_4\$ aque...](#)

[Figure 8.13 Some characteristics of 2G ARLBs. \(a\) Schematic illustration of ...](#)

[Figure 8.14 \(a\) Charge/discharge curves for 100% DOD of the Li//Br battery a...](#)

[Figure 8.15 \(a\) CV curves of Zn and \$\text{Na}_{0.95}\text{MnO}_2\$ in an aqueous solution of 0.5...](#)

[Figure 8.16 \(a\) Charge and discharge curves and \(b\) cycling performance of L...](#)

[Figure 8.17 Charge and discharge curves of \$\text{Li}\[\text{Ni}_{0.8}\text{Co}_{0.1}\text{Mn}_{0.1}\]\text{O}_2\$ \(811\) prepa...](#)

[Figure 8.18 Cycling behavior of uncoated and coated \$\text{LiMn}_2\text{O}_4\$ at 50 °C.](#)

[Figure 8.19 Schematic illustration of the preparation process for three-dime...](#)

[Figure 8.20 Electrochemical performance of the porous \$\text{LiFePO}_4\$ prepared by a ...](#)

[Figure 8.21 Some structural parameters of a graphite crystal.](#)

[Figure 8.22 Formation of stage compounds when lithium is intercalated into g...](#)

[Figure 8.23 Charge/discharge curves of MCMB-2528 in a 1.0 M \$\text{LiPF}_6\$ -PC:DEC \(3 ...](#)

[Figure 8.24 Charge and discharge curves of \$\text{Li}_4\text{Ti}_5\text{O}_{12}\$ nanoparticle at the rat...](#)

[Figure 8.25 Molecular structures of some typical organic cosolvents for elec...](#)

[Figure 8.26 Molecular structures of some typical lithium salts for electroly...](#)

[Figure 8.27 SEM micrographs of some typical separators for electrolytes of l...](#)

[Figure 8.28 Schematic process to manufacture lithium-ion batteries.](#)

[Figure 8.29 Discharge curves based on different negative and positive electr...](#)

[Figure 8.30 \(a\) SEM micrograph of the GO-S nanocomposite after heat treatmen...](#)

[Figure 8.31 Schematic illustration of \(a\) the construction of the composite ...](#)

[Figure 8.32 Charge and discharge curves at different rates for Na//S battery...](#)

[Figure 8.33 The schematic preparation process for nanoporous Se.](#)

[Figure 8.34 \(a\) Schematic illustration of rechargeable magnesium battery bas...](#)

[Figure 8.35 Comparison of GLIB and LIB based on a mesophase pitch-based grap...](#)

[Figure 8.36 SEM micrographs of the prepared porous P\(VDF-HFP\) membrane: \(a\) ...](#)

[Figure 8.37 Charge and discharge performance of a battery based on Si/C/CP/P...](#)

[Figure 8.38 Discharge curves of a solid lithium-ion battery based on graphit...](#)

[Figure 8.39 \(a\) Discharge curves at different rates and \(b\) cycling behavior...](#)

[Figure 8.40 Electrochemical performance of three kinds of Li//air batteries:...](#)

[Figure 8.41 Charge and discharge curves for a solid Li//air battery: solid e...](#)

[Figure 8.42 Discharge and charge curves of a Na//O₂ at various current densi...](#)

[Figure 8.43 Charge and discharge curves of the Zn//air batteries using the c...](#)

[Figure 8.44 Simplified solid-state structure of \$\beta''\$ -alumina and mechanism of ...](#)

[Figure 8.45 Simplified phase diagram of the system Na₂S-S.](#)

[Figure 8.46 Schematic cross section of a sodium-sulfur battery.](#)

[Figure 8.47 Variation of rest voltage and operating voltage during charging ...](#)

[Figure 8.48 Experimental OCVs of sodium transition metal chloride accumulato...](#)

[Figure 8.49 Schematic cross section of a sodium-nickel chloride accumulator....](#)

[Figure 8.50 Discharge curve of a sodium-nickel chloride accumulator at end o...](#)

[Figure 8.51 Charge/discharge curve of a sodium-iron chloride accumulator at ...](#)

[Figure 8.52 Horizontal cross section of a \$\beta''\$ -alumina solid electrolyte.](#)

[Figure 8.53 Schematic cross section of an all-molten metal accumulator.](#)

Chapter 9

[Figure 9.1 Comparison of ideal \(maximum\) efficiencies \$\eta_{\text{theor}}\$ as given b...](#)

[Figure 9.2 Scheme of the Grove cell.](#)

[Figure 9.3 Pathways of dioxygen reduction.](#)

[Figure 9.4 Schematic of side-on dioxygen interaction with M \(Griffiths model...](#)

[Figure 9.5 Schematic of bridged dioxygen interaction with two M.](#)

[Figure 9.6 Schematic of end-on dioxygen interaction with M.](#)

[Figure 9.7 Dioxygen reduction pathways.](#)

[Figure 9.8 Three-phase boundaries establish in a pore of a hydrophilic and a...](#)

[Figure 9.9 Scanning electron microscope picture of a PTFE-bonded platinum-ca...](#)

[Figure 9.10 Schematic cross-section of a hydrophilic bilayer electrode.](#)

[Figure 9.11 Schematic setup of a typical fuel cell: 1., porous electrode \(ano...](#)

[Figure 9.12 Cell voltage and output power of a typical fuel cell.](#)

[Figure 9.13 Schematic cross-section of an alkaline fuel cell.](#)

[Figure 9.14 Molecular structure of sulfonated perfluorocarbon polymer.](#)

[Figure 9.15 Schematic cross section of the internal structure of sulfonated ...](#)

[Figure 9.16 Molecular structure of carboxylated perfluorocarbon polymer.](#)

[Figure 9.17 Schematic cross section of a single fuel cell with \(1\) bipolar p...](#)

[Figure 9.18 Platinum distribution along a cross section of an MEA obtained b...](#)

[Figure 9.19 Platinum distribution along a cross section of an MEA as obtaine...](#)

[Figure 9.20 Top view on platinum coating on MEA.](#)

[Figure 9.21 Top view of a layer of platinum black/PTFE pressed on top of a C...](#)

[Figure 9.22 Cross-sectional image and platinum distribution obtained with a ...](#)

[Figure 9.23 Top view of a layer of Ir:Ru/PTFE pressed on top of a CEM.](#)

[Figure 9.24 Platinum sputtered on titanium.](#)

[Figure 9.25 Platinum coating on a sintered titanium carrier obtained by vapo...](#)

[Figure 9.26 Operating scheme of a direct alcohol \(methanol\) fuel cell](#)

[Figure 9.27 Schematic cross section of a phosphoric acid fuel cell.](#)

[Figure 9.28 Schematic cross section of a molten carbonate fuel cell, Me = Li...](#)

[Figure 9.29 Cross-section of a tubular cell.](#)

[Figure 9.30 Arrangement of SOFCs.](#)

[Figure 9.31 Schematic operational principle of a fuel cell \(a\) and an electr...](#)

Chapter 10

[Figure 10.1 Scheme of an all-vanadium redox flow battery.](#)

[Figure 10.2 Scheme of a redox flow battery cell in a cell stack.](#)

[Figure 10.3 Taxonomy of redox flow batteries.](#)

[Figure 10.4 All-vanadium RFB, 8 kW maximum output, 10 kW maximum input, stor...](#)

[Figure 10.5 Structural formula of tetrachloro-*p*-benzoquinone.](#)

[Figure 10.6 The redox reaction at the positive electrode.](#)

[Figure 10.7 Scheme of a VSSB; \(1\) current collector, \(2\) carbon felt with VO...](#)

[Figure 10.8 Schematic layout of a vanadium-dioxygen system.](#)

Chapter 11

[Figure 11.1 Working principle of electrical double-layer capacitors: 1, 2, a...](#)

[Figure 11.2 Working principle of a pseudocapacitor: \$E_a\$, \$E_b\$, \$E_a + E_1\$, and \$E_b\$...](#)

[Figure 11.3 Working principle of hybrid capacitor.](#)

[Figure 11.4 CV curves of AC as negative electrodes in different aqueous elec...](#)

[Figure 11.5 \(a\) CV curves of a three-dimensional porous graphene at a scan r...](#)

[Figure 11.6 CV curves and galvanostatic charge/discharge curves of the three...](#)

[Figure 11.7 Galvanostatic charge/discharge curves of EDLCs consisting of mes...](#)

[Figure 11.8 Charge/discharge curves of an EDLC with positive and negative ac...](#)

[Figure 11.9 \(a\) The preparation scheme for RuO₂/GSs composites \(ROGS\), \(b\) C...](#)

[Figure 11.10 Schematic illustration of two key steps for preparing hybrid Mn...](#)

[Figure 11.11 CV curves of \(a\) MnO₂ in 0.5 M different neutral electrolytes a...](#)

[Figure 11.12 CV curves of AB and MnO₂/AB composite in 1 M LiClO₄ solution of...](#)

[Figure 11.13 Intrinsically conducting polymers suggested for use in supercap...](#)

[Figure 11.14 The different states of oxidation of PANI.](#)

[Figure 11.15 CVs of PANI at different scan rates in an aqueous 2.0 M H₂SO₄ e...](#)

[Figure 11.16 CV curves of PANI in \(a\) 1 M LiClO₄ aqueous solutions, \(b\) 1 M ...](#)

[Figure 11.17 CV curves of PPy: \(a\) rectangular-sectioned polypyrrole microtu...](#)

[Figure 11.18 Schematic illustration of the formation of PPy nanotube embedde...](#)

[Figure 11.19 CVs of PTH and its derivatives in organic electrolytes: \(a\) PTH...](#)

[Figure 11.20 CV curves of PEDOT in 1 M KCl solution at scan rate of 50 mV s⁻...](#)

[Figure 11.21 Variation of specific capacitance with current density in \(a\) 1...](#)

[Figure 11.22 Schematic illustration of the processes occurring on the carbon...](#)

[Figure 11.23 Reversible redox reactions between *o*-aminonaphthol \(**1**\) and *o*-na...](#)

[Figure 11.24 Ragone plot for the as-prepared GSs, RuO₂, and ROGCSs \(Ru, 38.3...](#)

[Figure 11.25 Electrochemical performance in 0.5 M K₂SO₄ electrolyte: \(a\) Rag...](#)

[Figure 11.26 Ragone plots of pseudocapacitors based on PEDOT-nanowires/carbo...](#)

[Figure 11.27 Electrochemical performance of a pseudocapacitor using carbon p...](#)

[Figure 11.28 Electrochemical performance of a pseudocapacitor based on PPy a...](#)

[Figure 11.29 Schematic illustration of the synthesis of \(a\) PPy@V₂O₅ nanobel...](#)

[Figure 11.30 \(a\) TEM micrograph of Ppy-coated MoO₃ nanorods, \(b\) CV curves o...](#)

[Figure 11.31 \(a\) Galvanostatic charge/discharge curves of the porous TiO₂ ho...](#)

[Figure 11.32 \(a\) Schematic illustration of three methods to prepare the comp...](#)

[Figure 11.33 \(a\) Typical charge/discharge curves of the three intercalation ...](#)

[Figure 11.34 \(a\) Illustration of the formation of the composite of \$\alpha\$ -MoO₃-de...](#)

[Figure 11.35 \(a\) CV curve of V₂O₅ nanowires and Ni mesh \(current collector\) ...](#)

[Figure 11.36 \(a\) Typical CV curves and \(b\) cycling performance of superlarge...](#)

[Figure 11.37 \(a\) CV curves of various electrodes at 50 mV s⁻¹ in 1 M K...](#)

[Figure 11.38 \(a\) CV curve of Ni\(OH\)₂ in alkaline solution and \(b\) charge/dis...](#)

[Figure 11.39 CV curves of LiCoO₂ and nickel mesh in saturated Li₂SO₄ solutio...](#)

[Figure 11.40 CV of LiNi_{1/3}Co_{1/3}Mn_{1/3}O₂ in 2 M Li₂SO₄ aqueous solution.](#)

[Figure 11.41 \(a\) SEM micrograph of the porous LiMn₂O₄ and \(b\) CV curve of th...](#)

[Figure 11.42 \(a\) CV curves of NaMnO₂ and K_xMnO₂ in 0.5 M Na₂SO₄ and K₂SO₄ aq...](#)

[Figure 11.43 Ragone plots of the hybrid capacitors: \(a\) V₂O₅//AC and PPy@V₂O](#)

[Figure 11.44 Electrochemical properties of the quasi-solid-state hybrid capa...](#)

[Figure 11.45 \(a\) Charge and discharge curves of AC, Li₄Ti₅O₁₂, and Li₄Ti₅O₁₂](#)

[Figure 11.46 \(a\) Schematic of the working mechanism of a sodium ion capacito...](#)

[Figure 11.47 EUCAR hazard level scale.](#)

[Figure 11.48 Working principle of supercapacitor \(SC\) as a power supply for ...](#)

[Figure 11.49 Photo of a bus \(No. 20\) in Shanghai, which was manufactured by ...](#)

[Figure 11.50 Advantages of energy storage for the electric power industry, e...](#)

Figure 11.51 Drive profile of a forklift powered by fuel cells and supercapa...

Electrochemical Energy Conversion and Storage

Yuping Wu and Rudolf Holze

WILEY-VCH

Authors

Prof. Dr. Yuping Wu

State Key Laboratory of
Materials-oriented Chemical
Engineering
School of Energy Science and
Engineering
Nanjing Tech University
Nanjing 211816
Jiangsu Province
China

Prof. Dr. Rudolf Holze

TU Chemnitz
Institut für Chemie
Straße der Nationen 62
09111 Chemnitz
Germany

All books published by **WILEY-VCH** are carefully produced. Nevertheless, authors, editors, and publisher do not warrant the information contained in these books, including this book, to be free of errors. Readers are advised to keep in mind that statements, data, illustrations, procedural details or other items may inadvertently be inaccurate.

Library of Congress Card No.: applied for

British Library Cataloguing-in-Publication Data

A catalogue record for this book is available from the British Library.

Bibliographic information published by the Deutsche Nationalbibliothek

The Deutsche Nationalbibliothek lists this publication in the Deutsche Nationalbibliografie; detailed bibliographic data are available on the Internet at <<http://dnb.d-nb.de>>.

© 2022 WILEY-VCH GmbH, Boschstr. 12, 69469 Weinheim, Germany

All rights reserved (including those of translation into other languages). No part of this book may be reproduced in any form – by photoprinting, microfilm, or any other means – nor transmitted or translated into a machine language without written permission from the publishers. Registered names, trademarks,

etc. used in this book, even when not specifically marked as such, are not to be considered unprotected by law.

Print ISBN: 978-3-527-33431-5

ePDF ISBN: 978-3-527-34028-6

ePub ISBN: 978-3-527-34029-3

oBook ISBN: 978-3-527-34030-9

Cover Design Adam-Design, Weinheim, Germany